



CHORUS

This is the accepted manuscript made available via CHORUS. The article has been published as:

Metastable states in the frustrated triangular compounds $\text{Ca}_{\{3\}}\text{Co}_{\{2-x\}}\text{Mn}_{\{x\}}\text{O}_{\{6\}}$ and $\text{Ca}_{\{3\}}\text{Co}_{\{2\}}\text{O}_{\{6\}}$

Jae Wook Kim, E. D. Mun, X. Ding, A. Hansen, M. Jaime, N. Harrison, H. T. Yi, Y. Chai, Y. Sun, S. W. Cheong, and V. S. Zapf

Phys. Rev. B **98**, 024407 — Published 9 July 2018

DOI: [10.1103/PhysRevB.98.024407](https://doi.org/10.1103/PhysRevB.98.024407)

Metastable states in frustrated triangular compounds $\text{Ca}_3\text{Co}_{2-x}\text{Mn}_x\text{O}_6$ and $\text{Ca}_3\text{Co}_2\text{O}_6$

Jae Wook Kim,^{1,2} E. D. Mun,^{1,3} X. Ding,¹ A. Hansen,^{1,4} M. Jaime,¹ N. Harrison,¹ H. T. Yi,² Y. Chai,⁵ Y. Sun,⁵ S. W. Cheong,² and V. S. Zapf¹

¹National High Magnetic Field Laboratory (NHMFL),

Los Alamos National Laboratory (LANL), Los Alamos NM 87545, USA

²Rutgers Center for Emergent Materials & Department of Physics and Astronomy, Piscataway, NJ 08854, USA

³Department of Physics, Simon Fraser University, Burnaby, B.C. V5A 1S6, Canada

⁴University of California Los Angeles, Westwood, CA, USA and

⁵Beijing National Laboratory for Condensed Matter Physics,

Institute of Physics, Chinese Academy of Sciences, Beijing 100190, P.R. China

(Dated: June 11, 2018)

The observation of unusual metastable behavior in $\text{Ca}_3\text{Co}_2\text{O}_6$ remains an ongoing puzzle. When the magnetic field is increased at certain very slow rates, evenly-spaced steps occur in the magnetization and other physical quantities as a function of magnetic field every 1.2 T. The ground state without steps is approached by a slow relaxation processes over hours to days. It is a striking example of extremely slow dynamics arising from geometrical frustration in an otherwise clean and long-range ordered system, and its precise description remains controversial. Here we shed light on the mystery by reporting similar behavior in isostructural $\text{Ca}_3\text{Co}_{2-x}\text{Mn}_x\text{O}_6$, albeit at magnetic field sweep rates that are six orders of magnitude faster than that in $\text{Ca}_3\text{Co}_2\text{O}_6$. We observe these steps not only in the magnetization, but also in the magnetostriction, electric polarization, and magnetocaloric effect. We present a study of metastable behavior in both compounds across seven orders of magnitude of magnetic field sweep rates using unique magnets at the National High Magnetic Field Laboratory. The metastable steps occur for intermediate ranges of magnetic field sweep rates, vanishing or evolving for the fastest and slowest sweep rates. Our data support that these metastable steps are an intrinsic feature of the three-dimensionally-frustrated geometry of Ising spins in this structural family and thus narrow the number of applicable models.

PACS numbers: 75.60.-d, , 75.60.Ej, 75.85.+t

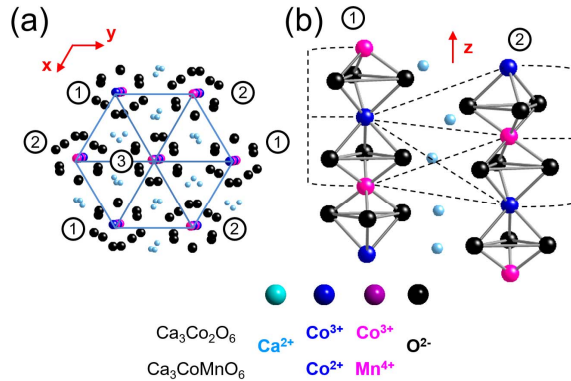


FIG. 1. (a) Crystal structure of $\text{Ca}_3\text{Co}_2\text{O}_6$ (CCO) and $\text{Ca}_3\text{CoMnO}_6$ (CCMO) showing the hexagonal ab plane. The indices 1, 2, 3 denote each of the three sublattices, which are c -axis chains containing alternating Co^{3+} $S = 2$ and $S = 0$ ions (CCO) or Co^{2+} and Mn^{4+} ions (CCMO). (b) Two chains viewed along the $[110]$ direction.

I. INTRODUCTION

Magnets with frustrated geometries can give rise to emergent slow dynamics and metastable states. The energy landscape of frustrated magnets contains many nearly-degenerate states, some with high entropy allowing for slow evolution of the physical properties and trapping into metastable excited states. This glassy-type behavior occurs despite the apparently clean geometry of these systems. For example, in spin ice materials, very slow relaxation of the magnetiza-

tion occurs that is modeled in terms of topological entanglement of monopole excitations, whose untangling dictates the timescale for relaxation¹⁻³. In other frustrated systems, the presence of dynamic excitations can stabilize static ordering in a system that would otherwise favor a spin liquid ground state⁴⁻¹¹. In general it is necessary to understand the dynamics of frustrated magnets in order to capture their essential behavior. We note that this field is of practical importance to quantum annealing computers that attempt to find the true ground state in an energy landscape of metastable traps, and whose Hamiltonians can be analogous to those of frustrated magnets¹².

Here we investigate dynamic behavior that emerges in the frustrated chain compounds $\text{Ca}_3\text{Co}_2\text{O}_6$ (CCO) and $\text{Ca}_3\text{CoMnO}_6$ with $0.97 \leq x \leq 1.03$ (CCMO). CCO provides a dramatic example of metastable magnetic behavior that has puzzled the community for several decades. This material forms c axis ferromagnetically coupled chains of Ising $S = 2$ Co^{3+} spins (every second Co^{3+} spin is $S = 0$), and these chains are in turn arranged in a triangular configuration in the ab plane with frustrated antiferromagnetic interactions. At 4 K, the magnetization vs magnetic field exhibits a plateau at $1/3$ of the saturation magnetization before leaping to the final saturation value. However for sweep rates faster than $d\mu_0 H/dt = 1.6 \times 10^{-4}$ T/s, a different magnetic behavior occurs, namely regular flat plateaus appear in $M(H)$ separated by regular steps every 1.2 T. For temperatures below 4 K, the relaxation times diverge and the $1/3$ plateau ground state is never reached in multiple day-long experiments^{13,14}. The metastable magnetization steps are reproduced in other

physical properties including elastic neutron diffraction peak intensities¹⁵. For much faster $d\mu_0 H/dt$ of 2 and 6.7 kT/s that are applied by capacitor-driven pulsed magnets, a polycrystal study finds that the number of magnetization steps is reduced compared to slower sweep rates and new dynamic behavior appears¹⁶.

Many detailed models have been advanced to explain the slow magnetic dynamics and regular metastable steps in $M(H)$ in CCO. The similarity of the metastable steps to those seen in single-molecule magnets has prompted suggestions of quantum tunneling within isolated chains of this compound^{13,14}. Another class of models predicts rigid ferromagnetic spin chains along the c axis that form successive metastable patterns in the triangular ab plane with increasing H ¹⁶⁻¹⁸. However, a recent single-crystal neutron diffraction study finds long-wavelength modulations ($\lambda \sim 1000$ Å) along the c axis chains, on top of a partially-disordered antiferromagnet ground state¹⁹⁻²¹. The wavelength varies continuously as a function of temperature (T) and relaxes slowly over time, not reaching equilibrium even after 13 hours at 8 K. These results are hallmarks of the classic axial next-nearest neighbor Ising (ANNNI) model²²⁻²⁴. This fact prompted a recent description²⁵ of the metastable steps using a modified version of this model: three chains in a triangle are treated as one chain with frustrated nearest-, next-nearest, and next-next-nearest-neighbor interactions, and these triple-chains are coupled ferromagnetically.

An experimental finding that is not captured by any models is spontaneous magnetic phase segregation. Neutron diffraction at $H = 0$ suggests coexisting long and short-range order²⁶ and a small-angle neutron scattering study resolves nanoscale ferromagnetic hexagonal clusters in the ab plane²⁷. The complete behavior of this system and the origin of metastable steps thus remains a puzzle.

Our second material, CCMO is isostructural to CCO, but the c axis chains contains alternating isotropic $S = 3/2$ Mn⁴⁺ spins and Ising-like $S = 3/2$ Co²⁺ spins (see Fig. 1)²⁸⁻³¹. Whereas CCO has a ferromagnetic Curie-Weiss temperature, CCMO has an antiferromagnetic one^{30,32,33}. Neutron diffraction studies of CCMO find that, in contrast to the modulated ferromagnetic behavior within the chains in CCO, the ground state in CCMO is an $\uparrow\uparrow\downarrow\downarrow$ arrangement of alternating Co²⁺ and Mn⁴⁺ spins along the chains^{29,34}, which is a structure that can result from frustration between nearest and next-nearest-neighbor interactions. This magnetic structures incidentally induces ferroelectricity via symmetric exchange striction, making this material multiferroic^{28,29,31}. Finally we note that a few percent off-stoichiometry of Mn and Co concentrations has been shown to be necessary to stabilize the long-range order, consistent with an order-by-disorder mechanism³⁴.

In this paper, we use seven orders of magnitude of magnetic field sweep rate $d\mu_0 H/dt$ to investigate the dynamic behavior of CCO and CCMO. We show that very surprisingly, CCMO also has metastable steps in the physical properties induced by finite sweep rate similar to those in CCO. However, the minimum magnetic field sweep rate $d\mu_0 H/dt$ required to induce the steps in CCMO is six orders of magnitude faster

than that in CCO. We observe these metastable behaviors reproducibly in multiple crystals, and in multiple properties: magnetization, electric polarization, magnetostriction, and the magnetocaloric effect. We use a uniquely tunable generator-driven long pulse 60 T magnet at the NHMFL, among others, to observe the speeds where the metastable steps onset and disappear. By observing similar nonequilibrium behavior in these two isostructural materials across very different dynamic ranges we find that the observed metastable behavior is a robust consequence of the geometrical frustration in these systems and thus narrows the range of models that can explain the observed behavior.

II. EXPERIMENTAL

Single-crystalline samples of CCO and CCMO were grown by the flux method and cut to typical dimensions of $0.5 \times 0.5 \times 3.0$ mm³²⁸. Three magnets were used to generate different $d\mu_0 H/dt$: 1) a 14 T superconducting (SC) magnet 2) a generator-driven 60 T long pulse magnet and 3) capacitor-driven short pulsed magnets with peak fields up to 65 T. Below 10 T, the sweep rates $d\mu_0 H/dt$ are 10^{-4} to 10^{-2} T/s (SC), 15 to 148 T/s (long pulse) and 1 to 4 kT/s (short pulse) as shown in Figs. 2(b), 3(g, h) and the Supplementary Information (S. I.)³⁵.

Physical properties were measured using a set of established measurement techniques for DC and pulsed magnetic fields that are appropriate for magnetic insulators³⁶⁻⁴⁰. Magnetization data in capacitor-driven pulsed magnets were measured using a compensated, sample-in/sample-out pickup-coil³⁶, and in 14 T superconducting magnets with a vibrating sample magnetometer (Quantum Design). The pulsed-field magnetization data were calibrated against magnetization measured in the superconducting magnet at temperatures above the regime where the metastable and hysteretic behavior occurs. Magnetostriction - the length change in response to magnetic fields - was also measured as it confirms the magnetization findings and is one of the most sensitive measurement techniques for detecting magnetic transitions in pulsed magnetic fields. It can be accurately determined for all different speeds of magnetic field sweep rate used here whereas magnetization only works well for the fastest and slowest sweep rates. Magnetostriction was thus measured in pulsed magnets using an optical fiber grating method^{37,38,40} and in superconducting magnets by a piezoelectric method⁴¹ as well as an optical fiber grating. Electric polarization changes $\Delta P(H)$ were also measured in CCMO since it has been previously investigated for multiferroic behavior and metastable steps were observed. In pulsed magnets electric polarization were obtained in CCMO by the standard technique of recording and integrating changes in the induced surface charge on silver-paint contacts on opposing ab faces of the sample, measured using a current amplifier, after poling in an electric field of 645 kV/m from 40 K³⁹. For CCMO, the magnetocaloric effect in the 60 T shaped pulsed magnet was measured with the sample attached to a thermally-insulating probe in vacuum while a magnetic field-calibrated resistance thermometer attached to

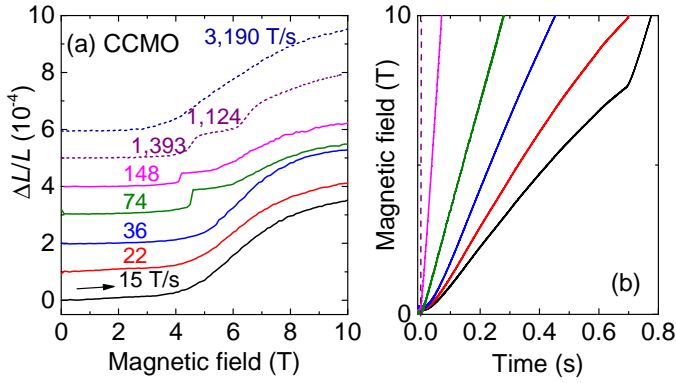


FIG. 2. (a) Magnetic field-dependence of c axis magnetostriction $\Delta L/L = [L(H) - L(0)]/L(0)$ during upsweeps with different sweep rates measured at $T = 1.4$ K for CCMO with $x = 0.97$. Sweep rates between 15 and 148 T/s are created by the generator-driven long pulse magnet (solid lines) while higher sweep rates are created by capacitor-driven short pulse magnets with 9 and 30 T peak fields (lower and upper dotted lines). Data are shifted vertically for clarity. (b) Magnetic field vs time of the long pulse magnet (solid lines) and short pulse magnet (vertically-appearing dashed lines) used to apply the magnetic fields in (a).

the sample recorded the temperature⁴². For CCO, the magnetocaloric effect was measured by monitoring the temperature with changing magnetic field with the sample mounted on the ⁴He heat capacity stage of a PPMS. All measurements are shown for the magnetic easy axes $H \parallel c$ while no metastable behavior was observed for $H \perp c$. This suite of techniques allows us to verify the bulk nature of the observed steps, rule out experimental artifacts, and track the dynamics across extended magnetic field sweep rates.

III. RESULTS

The magnetostriction data for CCMO are shown in Fig. 2 and demonstrates that the metastable steps occur for an intermediate range of $d\mu_0 H/dt$. The magnetostriction $\Delta L/L$ of CCMO with $x = 0.97$ is plotted as a function of H at different $d\mu_0 H/dt$ between 15 and 3,200 T/s. One or two sharp steps appear in $\Delta L/L$ for $d\mu_0 H/dt$ between 74 and 1,400 T/s below 12 T. On the other hand for slower and faster sweep rates, $\Delta L/L$ increases smoothly in this field range.

We observe similar step-like behavior in other physical properties of CCMO. In Fig. 3, the magnetization $M(H)$, electric polarization $\Delta P(H)$, magnetostriction $\Delta L/L$ and magnetocaloric effect $T(H)$ are shown for CCMO, for sweep rates where the steps occur. $T(H)$ was measured at 148 T/s in the long pulse magnet due to the need for thermalization time between the thermometer and the sample, while the other quantities are shown measured in a short pulse magnet with sweep rates up to 1,500 T/s. For comparison we show the same properties of CCO for sweep rates where the steps occur in that compound, namely 0.01 T/s at 2 K in a SC magnet.

For CCMO in Fig. 3 we find two jumps in the magnetiza-

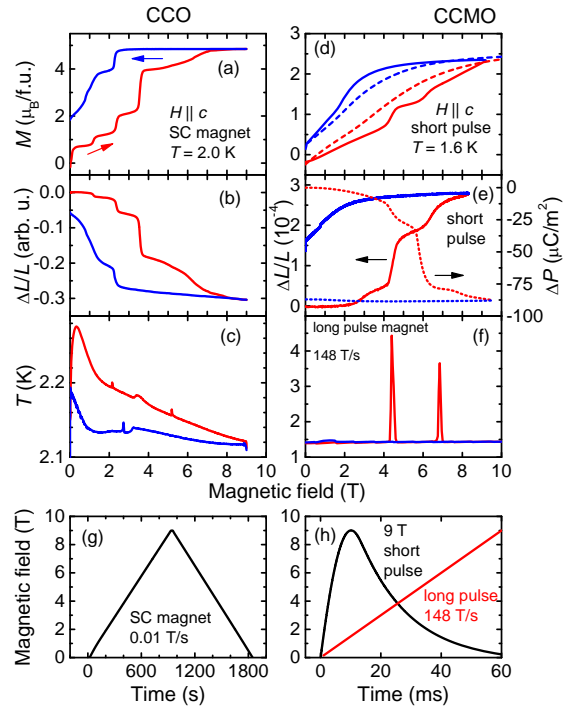


FIG. 3. Field-dependent properties of CCO in a superconducting (SC) magnet, and CCMO with $x = 0.97$ in pulsed magnets for $H \parallel c$. (a, d): c axis magnetization (M). (b, e): c axis magnetostriction ($\Delta L/L$), and (c, f) magnetocaloric effect $T(H)$. In (d), solid and dashed lines indicate pulsed field data and SC magnet data, respectively. In (e) the change of c axis electric polarization ($\Delta P \equiv P(H) - P(0)$, dotted lines) is also shown in the right scale. Red and blue lines indicate up and down sweep, respectively. (g): Time dependence of H for the SC magnet and (h) short pulse magnet ($d\mu_0 H/dt$ up to 1,500 T/s), and long pulse magnet with 148 T/s.

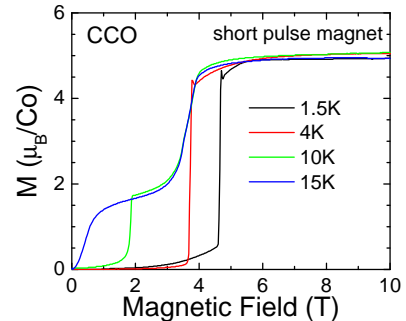


FIG. 4. Magnetization M vs magnetic field for CCO during an up-sweep of a 10 T magnetic field pulse ($d\mu_0 H/dt$ up to 1,660 T/s) at temperatures of 1.5, 4, 10, and 15 K. Applied magnetic field vs time and the sweep rate are shown in Fig. 3(h) and the S. I.³⁵.

tion at ~ 4 and 6 T in the up sweep and one anomaly at 1.5 T in the down sweep. The sweep rate $d\mu_0 H/dt$ corresponding to the jumps is 1,455 and 1,210 T/s at 4 and 6 T in the up sweep and 1 kT/s at 1.5 T on the down sweep. Similar steps are observed in the c axis magnetostriction and electric polarization measurements. The steps are no longer observed for a pulse with a peak sweep rate of 3,000 T/s. For low sweep rates in SC magnets with $d\mu_0 H/dt = 0.01$ T/s, the steps are also not observed: $M(H)$ for CCMO in a SC magnet is monotonic (dashed lines in Fig. 3(d)), as are other physical properties described in the literature²⁹.

Moving on to CCO in a SC magnet with 0.01 T/s, in Fig. 3 the magnetization $M(H)$ and the magnetostriction $\Delta L(H)/L$ show three small metastable steps at regular H intervals followed by a large, sweep-rate-independent step at 4 T. This is consistent with previous results^{13,17}. We note that the magnetostriction of CCO was negative with increasing fields for most of the CCO samples measured, positive for one sample, and inconsistently negative and positive for one sample. All CCO samples showed the steps in the magnetostriction, only the sign of the magnetostriction, varied, which may be due to sample dependence or strain effects⁴⁰. Upon decreasing H , M is constant until a sudden drop at 2 T and decreases to a remnant magnetization value at $H = 0$. The magnetocaloric effect data correspondingly show three peaks – two large and one small – on the upsweep and one small peak on the down sweep. Pulsed-field measurements of CCO were also performed in a short pulse magnet with a peak sweep rate of 1,500 T/s, as shown in Fig. 4. These measurements show that in CCO at these fast sweep rates only one step is selected for 1.5 and 4 K, and two steps for 10 and 15 K.

To summarize these results, the metastable steps in the physical properties of CCMO occur for sweep rates (measured at the field of the steps) between 74 and 1,400 T/s at 1.4 K, while for CCO steps onset above 1.6×10^{-4} T/s at 4 K^{13,14} and one or two steps persist up to 1,400 T/s depending on T . In fact the difference in sweep rates between the two compounds is even larger when considered at the same temperature. In CCO, the sweep rate required to create steps becomes slower than the measurement limit at 2 K.

In CCO, the metastable steps are evenly spaced in H ^{13,14} and occur below 4 T. In CCMO several roughly evenly spaced, metastable steps are found below 10 T. As the magnetic field is further increased past the region of metastable steps, both compounds show a sweep-rate-independent step toward saturation, at 8 and 21 T in CCO and CCMO, respectively. In CCO, this 8 T step leads to final saturation of the magnetization. In CCMO, the step at 21 T has been ascribed to the saturation of Ising-like Co^{2+} ($S = 3/2$) while the Mn^{4+} spins continue to evolve until 85 T³¹.

IV. DISCUSSION

The observation of metastable steps in multiple physical properties proves that they are intrinsic features of the magnetic systems. The fact that the steps occur in the two different compounds at very different sweep rates indicates that they

are a robust and general consequence of the geometrical frustration common to this structure class. Both materials feature a frustrated triangular lattice containing Ising-like Co spins. In CCMO, the presence of quasi-isotropic Mn^{4+} ions interspersed between Ising-like Co^{2+} spins may provide a mechanism for the much faster dynamics observed compared to CCO.

Below we discuss the implication of observing the steps in both CCO and CCMO for several theoretical models. First we note that the emergence of steps in CCMO cannot be due to CCO impurities within the CCMO sample because the size of the steps is macroscopic and reproducible for samples with three different compositions x as shown in the S. I.³⁵. Moreover, the steps in CCMO occur at different magnetic fields and dramatically different sweep rates compared to those in CCO.

Our results are also not consistent with models positing quantum tunneling within ferromagnetic chains of Ising spins, similar to quantum tunneling in single-molecule magnets^{13,14}. These models are already somewhat incompatible with the previous observation of long-wavelength modulation of the chains in CCO^{21,26}. However in CCMO the c axis chains form an $\uparrow\uparrow\downarrow$ antiferromagnetic state, not a ferromagnetic state, and thus a common quantum tunneling mechanism for the steps can be ruled out.

Our results do not support models relying on ferromagnetic chains forming different patterns in the ab plane^{16–18} since once again CCMO does not even have ferromagnetic chains.

The model that our results do support is a recent microscopic model based on the ANNNI model for CCO^{22,25}. Here it is found that similar values of the magnetization and local spin configurations can result from many different configurations of the frustrated triangular lattice. This degeneracy of states creates a high-entropy attractor and thus helps create a local minimum in the free energy corresponding to each metastable state²⁵. Both CCO and CCMO have ground states consistent with the ANNNI model, with different exchange interactions and thus these two compounds could have similar patterns of excited states within this model. In applied magnetic fields certain spin configurations have very high degeneracy due to the triangular lattice, and the high entropy of such states therefore creates a minimum in the free energy²⁵. This model has been shown to reproduce the magnetization steps at finite sweep rates in CCO²⁵. In CCMO, modifications of this model can also describe the observed behavior, however given the complexity of CCMO with two magnetic ions and many possible exchange paths, there is more than one possible model for the details of the exchange interactions that can describe the data⁴³. Thus it remains an unsolved challenge to converge on a single microscopic model for CCMO. Nevertheless, the observation of qualitatively similar dynamic behavior in these two triangular chain systems strongly supports the idea that the metastable steps are intrinsic features of this frustrated geometry.

The dynamic process of the observed metastable states in CCO and CCMO can be understood in terms of reaction rate theory^{44–47}. Two characteristic time scales are involved when the system enters into or escapes from a metastable state: relaxation time for the system to equilibrate with the local min-

imum and the escape time for the system to overcome the free energy barrier of the local minima. The relaxation time is determined by the shape of the local minima and the escape time is related to the shape of the local minima, magnitude of the energy barrier, and phenomenological friction coefficient when overcoming the free energy barrier^{44,46,47}. The magnetocaloric effect data supports this model of local metastable trapping as well. The magnetocaloric effect shows sudden irreversible heat release at the steps, consistent with a first-order process at the steps with an energy barrier⁴².

An open question is the spatial phase segregation that was observed at $H = 0$ in CCO²⁷. However these phase segregations were only observed at $H = 0$ and it would be unlikely for spontaneous magnetic phase segregation to produce such regular and reproducible steps in $M(H)$ in both compounds. Further measurements of phase segregation in applied H are necessary to further explore this issue.

Similar magnetization steps to CCO have also been observed in isostructural $\text{Sr}_3\text{Co}_2\text{O}_6$ ⁴⁸ though their dynamics have not been investigated. Another system in which such magnetic field sweep-rate dependence has been observed is a metal-organic Cu-based frustrated kagome system.⁴⁹ Here a metastable $1/3$ magnetization plateau was observed in pulsed-field magnetization M versus magnetic field H data that could only be accessed at certain magnetic field sweep rates $d\mu_0 H/dt$. This behavior was also attributed to a complex energy landscape that allows metastable trapping and relaxation to the ground state on certain timescales that compete with the magnetic field sweep rate⁴⁹.

V. SUMMARY

We investigate emergent metastable behavior in frustrated spin chain systems. We have used a uniquely broad range of tunable magnetic field sweep rates enabled by recent

magnet developments at the NHMFL to uncover that field-induced metastable steps occur in both CCO and CCMO. The metastable steps are qualitatively similar between CCO and CCMO, occurring at semi-regular H intervals and are suppressed at the extremes of high and low magnetic field sweep rates. However, the sweep rate that is required to trigger the steps in CCMO is at least six orders of magnitude faster than that in CCO. The presence of non-Ising-like Mn^{4+} interspersed between Ising-like Co^{2+} in CCMO is a likely source of faster relaxation times.

The presence of metastable steps and the common frustrated triangular geometry of these two compounds supports the concept that these steps are a general consequence of the frustration present in this isostructural family's geometry. The observation of steps across this set of measurement techniques confirms the bulk character of the steps. Within the frustrated geometry of these systems, consisting of chains that are antiferromagnetically coupled in the triangular a-b plane, it could be possible to create excited states with high degeneracy and/or local energy minima that entrap the system. Consequently, despite the different ground states of CCO and CCMO, a common metastable behavior can be induced by finite magnetic sweep rates. Our results are consistent with a recent model describing these materials in terms of a modified ANNNI model in which metastable states correspond to highly degenerate configurations of the triangular system²⁵.

ACKNOWLEDGMENTS

Work at LANL was funded by the LDRD program under the auspices of the U.S. DOE. Work at Rutgers was supported by the DOE under DE-FG02-07ER46382. The NHMFL facility is funded by the U.S. NSF Cooperative Grant No. DMR1157490 and DMR, the U.S. DOE, and the State of Florida. We thank Gia-Wei Chern, Yoshitomo Kamiya, and Cristian Batista for insightful discussions.

-
- ¹ L. Balents, *Nature* **464**, 199 (2010).
² L. D. C. Jaubert and P. C. W. Holdsworth, *Nat. Phys.* **5**, 258 (2009).
³ S. R. Giblin, S. T. Bramwell, P. C. W. Holdsworth, D. Prabhakaran, and I. Terry, *Nat. Phys.* **7**, 252 (2011).
⁴ J. Villain, R. Bidaux, J. P. Carton, and R. J. Conte, *J. Phys. Paris* **41**, 1263 (1980).
⁵ E. F. Shender, *Sov. Phys. JETP* **56**, 178 (1982).
⁶ A. G. Gukasov, T. Bruckel, B. Dorner, V. P. Plakhty, W. Prandtl, E. F. Shender, and O. P. Smirnov, *Europhys. Lett.* **7**, 83 (1988).
⁷ J. T. Chalker, P. C. W. Holdsworth, and E. F. Shender, *Phys. Rev. Lett.* **68**, 855 (1992).
⁸ T. Bruckel, B. Dorner, A. G. Gukasov, and V. P. Plakhty, *Phys. Rev. Lett. A* **162**, 357 (1992).
⁹ A. M. Turner, R. Barnett, E. Demler, and A. Vishwanath, *Phys. Rev. Lett.* **98**, 190404 (2007).
¹⁰ M. E. Zhitomirsky, M. V. Gvozdkova, P. C. W. Holdsworth, and R. Moessner, *Phys. Rev. Lett.* **109**, 077204 (2012).
¹¹ L. Savary, K. A. Ross, B. D. Gaulin, J. P. C. Ruff, and L. Balents, *Phys. Rev. Lett.* **109**, 167201 (2012).
¹² A. Das and B. Chakrabarti, *Rev. Mod. Phys.* **80**, 1061 (2008).
¹³ V. Hardy, M. R. Lees, O. A. Petrenko, D. M. Paul, D. Fluhaut, S. Hébert, and A. Maignan, *Phys. Rev. B* **70**, 064424 (2004).
¹⁴ A. Maignan, V. Hardy, S. Hebert, M. Drillon, M. R. Lees, O. Petrenko, D. M. K. Paul, and D. Khomskii, *J. Mater. Chem.* **14**, 1231 (2004).
¹⁵ C. L. Fleck, M. R. Lees, S. Agrestini, G. J. McIntyre, and O. A. Petrenko, *Euro. Phys. Lett.* **90**, 67006 (2010).
¹⁶ H. Kageyama, K. Yoshimura, K. Kosuge, M. Azuma, M. Takano, H. Mitamura, and T. Goto, *J. Phys. Soc. Jpn.* **66**, 3996 (1997).
¹⁷ Y. B. Kudasov, *Phys. Rev. Lett.* **96**, 027212 (2006).
¹⁸ X. Y. Yao, S. Dong, and J.-M. Liu, *Phys. Rev. B* **73**, 212415 (2006).
¹⁹ S. Agrestini, L. C. Chapon, A. Daoud-Aladine, J. Schefer, A. Gukasov, C. Mazzoli, M. R. Lees, and O. A. Petrenko, *Phys. Rev. Lett.* **101**, 097207 (2008).
²⁰ S. Agrestini, C. Mazzoli, A. Bombardi, and M. R. Lees, *Phys. Rev. B* **77**, 140403 (2008).

- ²¹ T. Moyoshi and K. Motoya, *J. Phys. Soc. Jpn* **80**, 034701 (2011).
- ²² P. Bak, *Rep. Prog. Phys.* **45**, 587 (1982).
- ²³ W. Selke, *Phys. Rep.* **170**, 213 (1988).
- ²⁴ L. C. Chapon, *Phys. Rev. B* **80**, 172405 (2009).
- ²⁵ Y. Kamiya and C. D. Batista, *Phys. Rev. Lett.* **109**, 067204 (2012).
- ²⁶ S. Agrestini, C. L. Fleck, L. C. Chapon, C. Mazzoli, A. Bombardi, M. R. Lees, and O. A. Petrenko, *Phys. Rev. Lett.* **106**, 197204 (2011).
- ²⁷ K. Prša, M. Laver, M. Månsson, S. Guerrero, P. Derlet, I. Živković, H. Yi, L. Porcar, O. Zaharko, S. Balog, J. Gavilano, J. Kohlbrecher, B. Roessli, C. Niedermayer, J. Sugiyama, C. Garcia, H. Rønnow, C. Mudry, M. Kenzelmann, S.-W. Cheong, and J. Mesot, “Magnetic nano-fluctuations in a frustrated magnet,” *ArXiv:1404.7398*.
- ²⁸ Y. J. Choi, H. T. Yi, S. Lee, Q. Huang, V. Kiryukhin, and S.-W. Cheong, *Phys. Rev. Lett.* **100**, 047601 (2008).
- ²⁹ Y. J. Jo, S. Lee, E. S. Choi, H. T. Yi, W. Ratcliff, Y. J. Choi, V. Kiryukhin, S. W. Cheong, and L. Balicas, *Phys. Rev. B* **79**, 012407 (2009).
- ³⁰ H. Wu, T. Burnus, Z. Hu, C. Martin, A. Maignan, J. C. Cezar, A. Tanaka, N. B. Brookes, D. I. Khomskii, and L. H. Tjeng, *Phys. Rev. Lett.* **102**, 026404 (2009).
- ³¹ J. W. Kim, Y. Kamiya, E. D. Mun, M. Jaime, N. Harrison, J. D. Thompson, V. Kiryukhin, H. T. Yi, Y. S. Oh, S.-W. Cheong, C. D. Batista, and V. S. Zapf, *Phys. Rev. B* **89**, 060404(R) (2014).
- ³² V. G. Zubkov, G. V. Bazuev, A. P. Tyutyunnik, and I. F. Berger, *J. Solid State Chem.* **160**, 293 (2001).
- ³³ M. Y. Ruan, Z. W. Ouyang, S. S. Sheng, X. M. Shi, Z. C. Xia, and G. H. Rao, *J. Magn. Magn. Mater.* **341**, 118 (2013).
- ³⁴ V. Kiryukhin, S. Lee, W. Ratcliff, Q. Huang, H. T. Yi, Y. J. Choi, and S.-W. Cheong, *Phys. Rev. Lett.* **102**, 187202 (2009).
- ³⁵ Supplementary Information contains the sweep rates and field profiles of the magnets used in this study, the temperature-dependence of the magnetization of CCMO in different magnets, the δ -dependence of the steps in the magnetization of CCMO, and additional sample preparation and measurement details.
- ³⁶ J. A. Detwiler, G. M. Schmiedeshoff, N. Harrison, A. H. Lacerda, J. C. Cooley, and J. L. Smith, *Phys. Rev. B* **61**, 402 (2000).
- ³⁷ R. Daou, F. Weickert, M. Nicklas, F. Steglich, A. Haase, and M. Doerr, *Rev. Sci. Inst.* **81**, 033909 (2010).
- ³⁸ M. Jaime, R. Daou, S. A. Crooker, F. Weickert, A. Uchida, A. Feiguin, C. D. Batista, H. A. Dabkowska, and B. D. Gaulin, *Proc. Nat. Acad. Sci.* **109**, 12404 (2012).
- ³⁹ V. S. Zapf, M. Kenzelmann, F. Wolff-Fabris, F. Balakirev, and Y. Chen, *Phys. Rev. B* **82**, 060402(R) (2010).
- ⁴⁰ M. Jaime, C. C. Moya, F. Weickert, V. Zapf, F. F. Balakirev, M. Wartenbe, P. F. S. Rosa, J. B. Betts, S. A. Crooker, G. Rodriguez, and R. Daou, *Sensors* **17**, 2572 (2017).
- ⁴¹ Y. F. P. R. Z. Levitin, V. N. Milov and V. V. Snegirev, *Physica B* **177**, 59 (1992).
- ⁴² V. S. Zapf, M. Jaime, and C. D. Batista, *Rev. Mod. Phys.* **86**, 563 (2013).
- ⁴³ Yoshitomo Kamiya, RIKEN, Japan, Personal communication.
- ⁴⁴ H. A. Kramers, *Physica* **7**, 284 (1940).
- ⁴⁵ S. Chandrasekhar, *Rev. Mod. Phys.* **15**, 1 (1943).
- ⁴⁶ P. Hanggi, *J. Stat. Phys.* **42**, 105 (1985).
- ⁴⁷ P. Hänggi, P. Talkner, and M. Borkovec, *Rev. Mod. Phys.* **62**, 251 (1990).
- ⁴⁸ X. X. Wang, J. J. Li, Y. G. Shi, Y. Tsujimoto, Y. F. Guo, S. B. Zhang, Y. Matsushita, M. Tanaka, Y. Katsuya, K. Kobayashi, K. Yamaura, and E. Takayama-Muromachi, *Phys. Rev. B* **83**, 100410 (2011).
- ⁴⁹ Y. Narumi, K. Katsumata, Z. Honda, J.-C. Domenge, P. Sindzingre, C. Lhuillier, Y. Shimaoka, T. C. Kobayashi, and K. Kindo, *Europhys. Lett.* **65**, 705 (2004).